



## A Review: Coffee and Tea Potential Materials for Carbonaceous Material Synthesis

Tutik Setianingsih

Department of Chemistry, Brawijaya University, Jl. Veteran 169 Malang 65145, Indonesia



### Abstract

Coffee and tea are classified as the biomass due to their characteristic lignocellulosic main content, including lignin, cellulose, and hemicellulose. However, their each most content is cellulose and lignin, respectively. Both coffee and tea have been used for preparation of biochar, activated carbon, and CNM/CNS. Biochar and activated carbon (AC) have different chemically structure, especially related to oxy groups and hydrocarbon aliphatic chain. CNM can has same or different crystal structure with activated carbon depend on the preparation way. As the adsorbent, activated carbon had higher average specific surface area (11x) and higher average pore volume (6X) than biochar. In other side, it had higher average specific surface area (4X) but same average pore volume compared to CNT. Using 3 different activators ( $\text{H}_3\text{PO}_4$ , KOH,  $\text{CO}_2$ ), hydrothermal pyrolysis produced the activated carbon which had 86X higher specific surface than without activator. In other side, it gave 6X higher specific surface area than slow pyrolysis method with those 3 activators. For the same metal cation adsorbate ( $\text{Cu}^{2+}$ ), each maximum adsorption ratio of AC to biochar, AC to CNT, and NaOCl-modified CNT to AC was about 2.4. For 4 different metal cations ( $\text{Cu}^{2+}$ ,  $\text{Ni}^{2+}$ ,  $\text{Pb}^{2+}$ ,  $\text{Cd}^{2+}$ ), the average maximum adsorption ratio of the functionalized CNT to AC was about 3.2.

**Key words:** Biochar; activated carbon; carbon nanomaterial; carbon nanostructure; coffee; tea.

### 1. Introduction

Coffee and tea are 2 drink types which are popular in Indonesia due to their characteristic tastes and colors. Even tea is one of the most drinks in the world, with a consumption in 2020 about 6.3 billion kilograms and estimated about 7.4 billion kilograms at 2025 [1]. Both materials have been used to prepare biochar [2-5], activated carbon [6-9], and CNM/CNS [10-13]. The chemical reasons why coffee and tea can be used as the carbon precursors are discussed in this paper.

Biochar, activated carbon, and CNM are the porous materials which have different porosity and surface functional groups as consequence of the different synthesis methods. Comparison of application for the three materials are given to understand how effect of their properties toward their different performances. The different synthesis methods are also described to give the real examples.

### 2. Tea and coffee as biomass sources of carbon precursor

Biomass is an organic complexe or organic solid product of organism and provided in the nature. Various waste such as manure, pulp waste, lumpur, various industry waste can be categorized as biomass because they can be processed to be energy. Generally, biomass is derived from product fraction which is biodegradable, agriculture waste, animal, fishery, and aquaculture [14]. Biomass or called bioresource is all organic substances derived from green plants which their molecules are destroyed after processes of digestion, burning, or decomposition [15]. Biomass is an organic material obtained from the photosynthesis process, either in the form of products or waste [16]. Tea is one of biomass sourcess, including tea leaves [17-20], stem, branches, and roots [21]. Coffee is also the biomass source, including spent coffee grounds [7,22], coffee dreg [16], coffee residue [23], coffee husk, mucilage, parchment, and silverskin [24].

The main contents of biomassa is cellulose, hemicellulose, and lignin, i.e. 40-60%, 10-30%, 20-30%, respectively [14]. Coffee dregs (*Coffea arabica* L.) contains hemicellulose which is composed of mannose (21.2%), galactose (13.8%), and arabinose (1.7%), also cellulose which consists of glucose (8.6% b/b). Coffee dregs also contain proteins (glutamic acid, leucine, glycine, valine, phenylalanine, alanine) and ash minerals, such as potassium, phosphorus, magnesium, and calcium [16]. As general biomass, coffee waste contain lignocellulosic substances with the highest cellulose amount of cellulose [24]. Tea leaves are composed of cellulose, hemicellulose, lignin, polyphenols, and proteins [4]. Among all those chemical contents, the lignocellulosic substances (lignin, hemicellulose, and cellulose) which are important for carbon preparations. Even each lignin [25-29], cellulose [30-33], and hemicellulose [34] have been used individually as carbon precursors for synthesis of carbonaceous materials. The lignocellulosic contents in various coffee and tea biomass are listed in Table 1 and Table 2, respectively. Based on both table the most average content in coffee and tea are cellulose and lignin, respectively. Lignin, cellulose, and hemicellulose have different range temperatures of thermal reactions in pyrolysis process, including dehydration, degradation and decarbonization reactions [35]. These different thermal characteristics make them create different characteristics of the

\*Corresponding author e-mail: [tutikimia88@gmail.com](mailto:tutikimia88@gmail.com) (Tutik Setianingsih)

Receive Date: 31 December 2024, Revise Date: 20 March 2025, Accept Date: 24 March 2025

DOI: 10.21608/ejchem.2025.349201.11078

©2025 National Information and Documentation Center (NIDOC)

carbon products. For example, individually lignin produced the biochar which had more C=O and C-O functional groups and much more percentage yield at the same pyrolysis temperature range of 500 – 800°C than cellulose [36].

**Table 1: Lignocellulosic contents in coffee biomass**

No.	Coffee biomass	% Cellulose	% Lignin	% Hemicellulose	References
1.	Pure SCG	49.8	31.9	15.4	[46]
2.	Blended SCG	48.9	36.7	10.5	[46]
3.	Spent coffee ground	47.3	29.3	19.0	[46]
4.	Spent coffee ground	47.3	24.6	19	[47]
5.	Coffee husk	43.0	9.0	7.0	[46, 48]
6.	Coffee cherry	27.6	13.7	12.5	[24]
7.	Coffee husk	43	9	7	[24]
8.	Spent coffee ground	23.6	17.8	12.1	[24]

**Table 2: Lignocellulosic contents in tea biomass**

No.	Tea biomass	% Cellulose	% Lignin	% Hemicellulose	References
1.	SGT	21.5	32.7	34.0	[46]
2.	Tea waste	25.4	25.7	31.1	[46]
3.	Green tea	14.26	52.44	33.33	[49]
5.	Black tea	28.13	61.34	10.53	[49]

### 3. Definition

Biochar is a solid which is rich of carbon atoms and produced by pyrolysis or carbonization of biomass without or limited oxygen gas. The activated biochar is the biochar which is prepared by involving activation process [14]. Biochar is a carbon-rich solid material produced by thermal decomposition of diverse waste biomass species under oxygen limited conditions [37]. Biochar is a porous carbonaceous solid material with a high aromatization degree, high decomposition resistance, formed by thermal breakdown of plant or animal biomass in thermal decomposition without oxygen [38]. Biochar is a carbonaceous material obtained by pyrolysis biomasses such as wood waste, sewage sludge, plant leaves, and crop residues, using an inert atmosphere or oxygen-free [39].

Biochar is obtained by biomass pyrolysis, whereas activated carbon is produced by chemical or physical activation of the biochar [40]. Activated biochar is biochar which is prepared by involving activation process [14]. Therefore, activated biochar and activated carbon is same material. Carbon nanomaterial (CNM) or carbon nanostructure (CNS) is a carbon material which has particle size of 1–100 nm [41,42].

### 4. Characteristics

There are differences of biochar, activated carbon, and CNM properties. First, based on material solid particle size, the biochar and activated carbon are not nanomaterials, whereas CNM is the nanomaterial. Nanomaterial can be verified by several methods, including dispersion test : the nanomaterial will be dispersed [11]. However, the activated carbon can be changed to CNM by grinding, blending, mixing, stirring or sonicating. Formation as colloid is needed for application of the CNM/CNS as the additive in fertilizer solution to make easy to spread it on the farm land [10-12,43]. The other methods are XRD by calculating the crystallite size based on FWHM, SEM and TEM through particle size on their images [41].

The second difference is about the crystal structure. Both biochar and activated carbon are mixture of amorph and graphite structure. Graphite is a carbon structure which is constructed by layers of graphene with space between layer is 3.35 Angstrom. In other side, the amorphous carbon has space between layer of 3.44 Angstrom [44]. Those spaces can be detected from d-spacing of the main peak of the activated carbon diffractograms [41]. Imagination about graphite and amorphous carbon are presented in Figure 2 based on HRTEM images in Figure 3. CNM has various crystal structures such as graphene, CNT, CNF, CND, CNH, fullerene, etc. The CNM structures are presented in Figure 4.

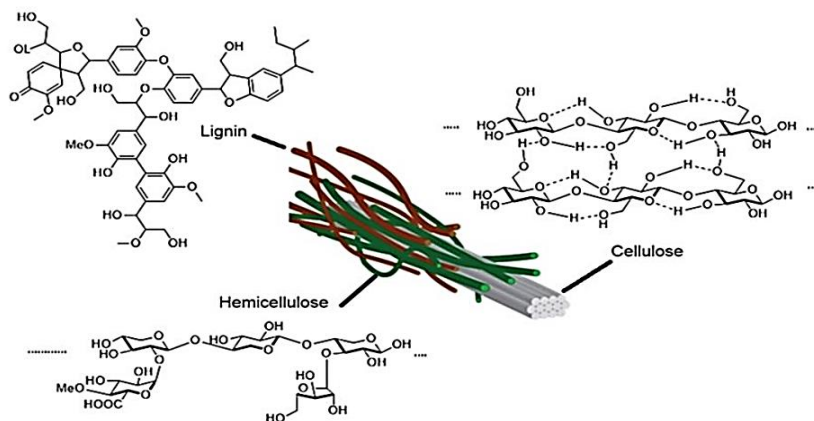


**Fig. 1. Lignocellulosic substances in biomass [45].**

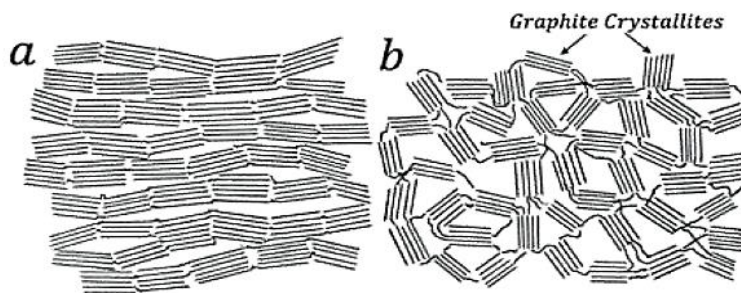


Fig.2. Structure of graphite and non graphite [50].

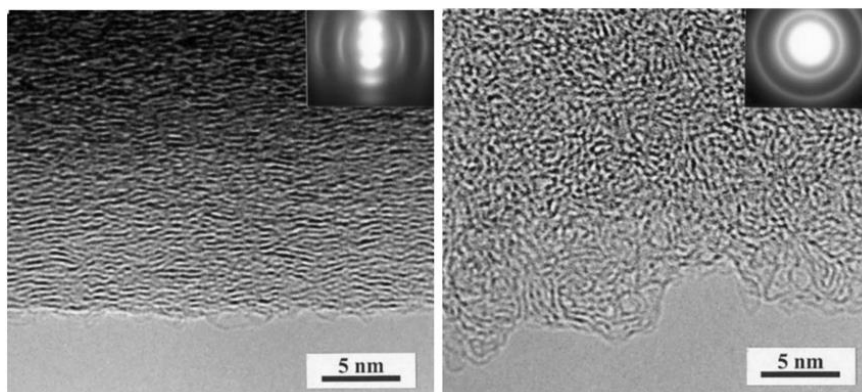


Fig. 3. HRTEM images of antrachen based graphite and sucrose based non graphite [51]

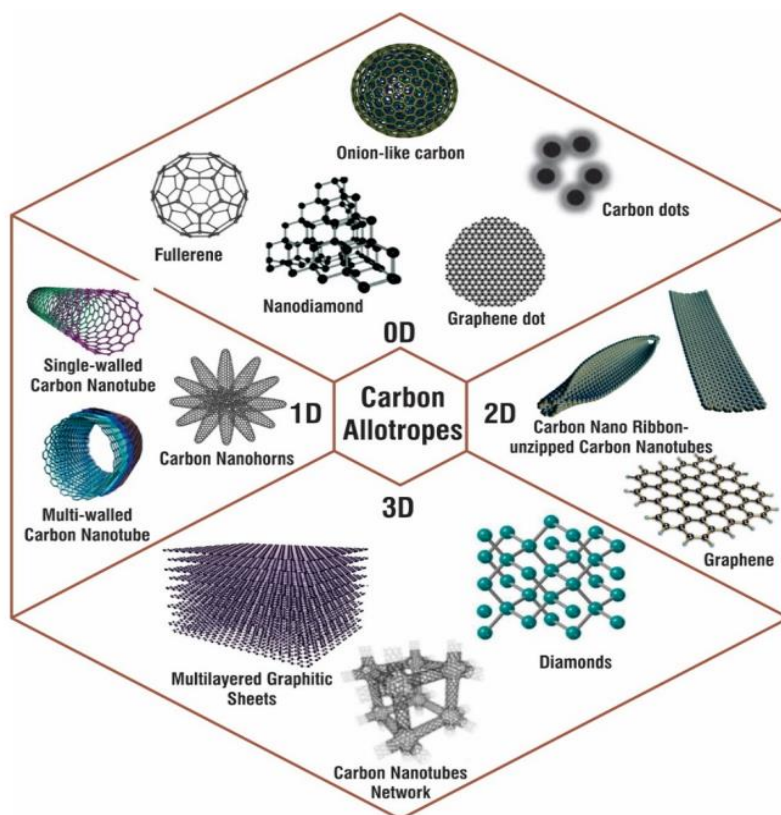


Fig. 4. CNM atom models in various dimension [52].

Based on surface area, AC is a carbonaceous material with better pore structure, larger specific surface area than biochar as the consequence of activation treatments, including physical activations and chemical activations [53]. Among all chemical activators, potassium hydroxide (KOH) is one of the most effective for obtaining large surface area of carbons. For example the activated carbon from birch wood by KOH activation using tube furnace under nitrogen gas stream had  $S_{\text{BET}}$  of 3160  $\text{m}^2/\text{g}$  [54]. The activated carbons from spruce cone, silver spruce cone and full spruce cone with KOH activator, same tube furnace under argon stream have large specific surface area (SSA) of 3565, 3497, and 3067  $\text{m}^2/\text{g}$ , respectively [55]. However, the opinion about KOH is right for slow pyrolysis, but not for hydrothermal pyrolysis [53] as listed in Table 3.

**Table 3: Effect of activator toward porosity of the activated carbon**

Pyrolysis type	Activator	$S_{\text{BET}}$ ( $\text{m}^2/\text{g}$ )	$V_p$ ( $\text{cm}^3/\text{g}$ )	References
Hydrothermal	No activator	23.1	0.1175	[53]
	$\text{H}_3\text{PO}_4$	2595	1.625	[53]
	KOH	857	0.3435	[53]
	$\text{CO}_2$	2475	0.1445	[53]
Slow pyrolysis	No activator	13.7	0.006	[53]
	$\text{H}_3\text{PO}_4$	357	0.1565	[53]
	KOH	1325	0.483	[53]
	$\text{CO}_2$	343	0.142	[53]

Lower surface area obtained by usage of KOH as the chemical activator in hydrothermal method is probably related to presence of water solvent which dissolve the KOH and lower temperature of hydrothermal method which is impossible to make dry condition in the autoclave. Both makes KOH can not worked as well as in the dry pyrolysis as the template of pore. In other side, phosphoric acid and  $\text{CO}_2$  worked better in presence of water solvent in chemical activation reaction than worked as the pore template.

Comparison of specific surface area and pore volume for the 3 different carbons can be seen in Table 4. Table 4 shows that CNM (CNT type) has larger specific surface area than biochar. It is probably caused by smaller size of solid particle. However, compared to activated carbon CNT have much lower specific surface area than activated carbon. It is possibly also caused the much smaller solid particle size which unfortunately reduces pore numbers due to destructed pores by reducing of solid particle.

**Table 4: Specific surface area and pore volume of CNT, biochar and activated carbon**

No.	Carbon type	SSA ( $\text{m}^2/\text{g}$ )	$V_p$ ( $\text{cm}^3/\text{g}$ )	References
1.	MWCNT	175	0.664	[56]
2.	SWCNT	557	1.043	[56]
3.	Biochar (1)	85	0.057	[56]
4.	Biochar (2)	142	0.185	[56]
5.	Powder Activated Carbon	1255	0.757	[56]
6.	Granule Activated Carbon	1354	0.778	[56]

Chemically, biochar has both lower oxygenated functional group density and higher content of aliphatic hydrocarbon probably due to incomplete cellulose and lignin combustion. Activation makes formation of more aromatic structure and oxygenated functional groups on activated carbon, as shown in Figure 5 and 6.

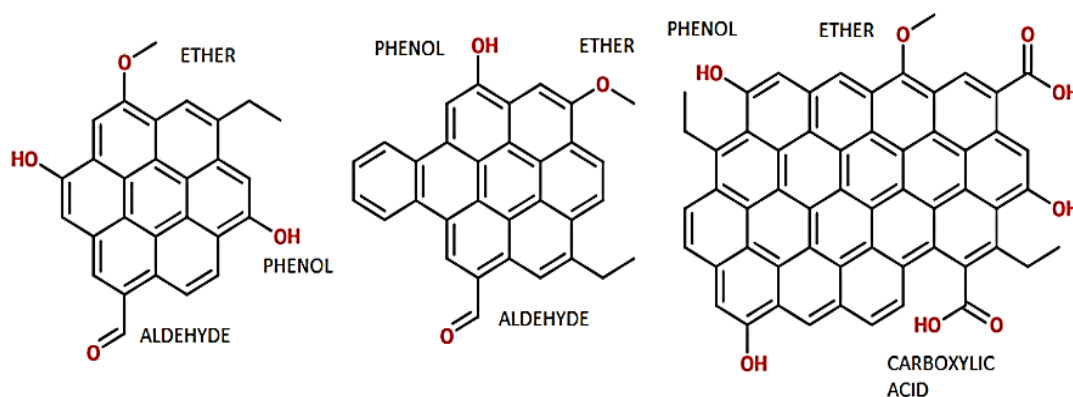


**Fig. 5. Structure of biochar based on different temperature and pyrolysis type , from left to right: fast pyrolysis 500°C, slow pyrolysis 500°C, gasification 760°C [57].**



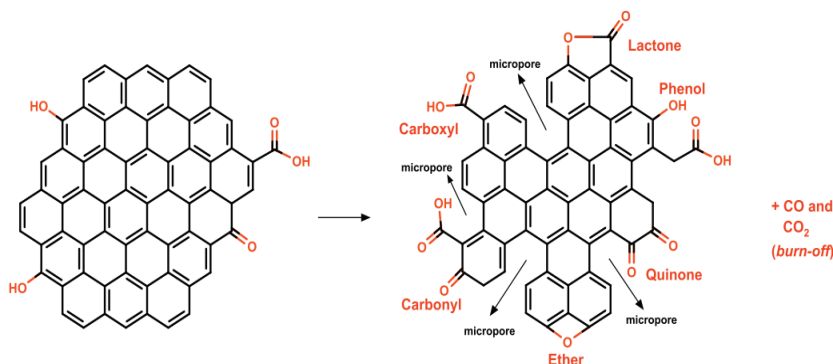


Fig. 6. Improvement of functional group before and after thermal air oxidation [58].

Number of aromatic structure in biochar also is affected by production route. Thermal pyrolysis route gives higher density of aromatic structure than hydrothermal pyrolysis, such as shown by Figure 7 and 8. Dry pyrolysis tends to work better in formation of the aromatic structure network than hydrothermal. Principally, presence of  $H_2O$  in the hydrothermal pyrolysis can make the activator enter into all part of the precursor. However higher temperature in the dry pyrolysis makes the thermal reactions and the pore templating in dry pyrolysis process more effective than in the hydrothermal one.

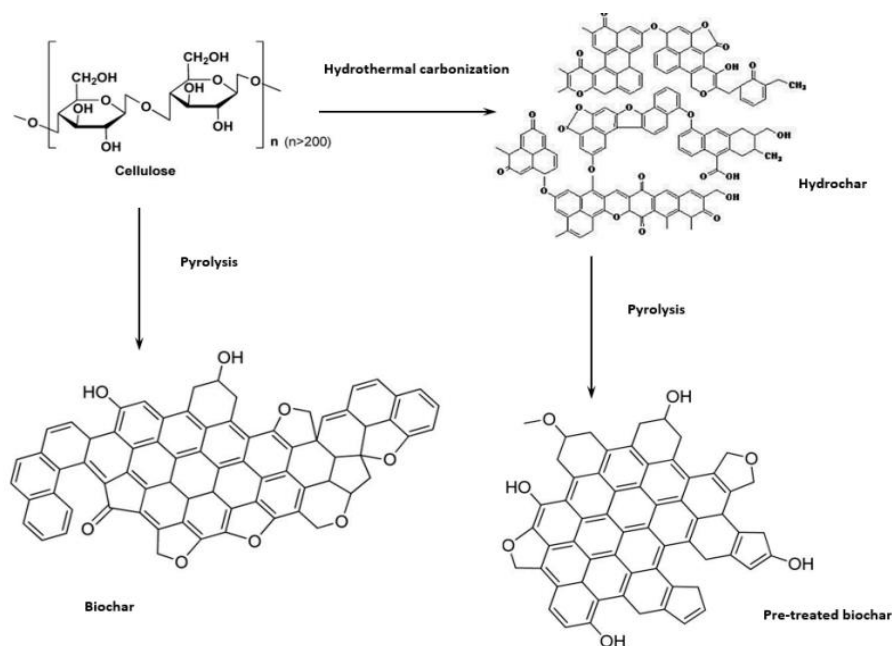


Fig. 7. Structure of biochar based on different method : thermal pyrolysis VS hydrothermal pyrolysis followed thermal pyrolysis [59].

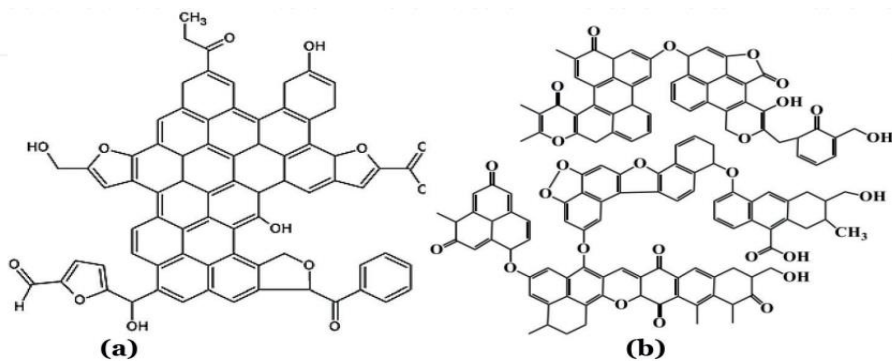


Fig. 8. Chemical structure : a) pyrochar and b) hydrochar [60].

The surface area of biochar are also affected by the pyrolysis temperature. The formation of microstructure and surface area of biochar increase by increasing pyrolysis temperature. The opened internal structure of biochar was observed for pyrolysis temperature  $\geq 450$  °C [61]. For example, by using miscanthus as the feedstock, the surface area of the biochar increased from 2.41 to 382 m<sup>2</sup>/g by increasing of temperature from 400 to 600°C [62]. With same tendency but higher value is about activated carbon, using blue coke powder precursor, the surface area improved from 75.50 to 636.91 m<sup>2</sup>/g and total pore volume of 0.059 to 0.363 cm<sup>3</sup>/g for increasing of temperature from 500 to 1000°C [63]. Fig 9 describe that temperature affected the pore and oxy functional group formation. For range temperature more than 450°C, the higher temperature the larger numbers of the pore and oxy groups the less remain unpyrolyzed organic substances.

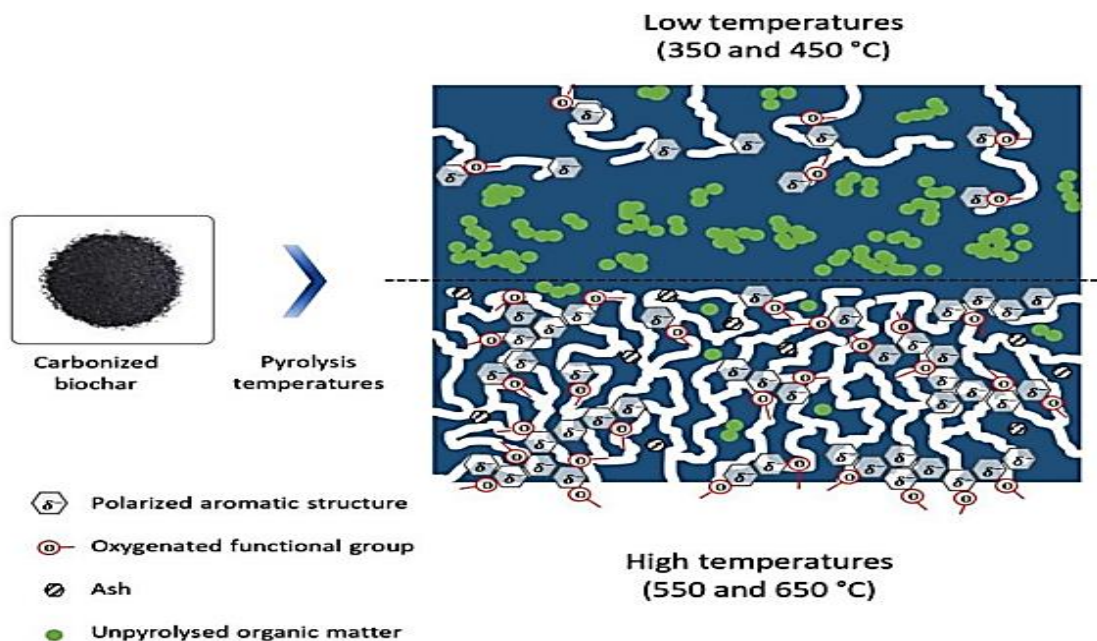


Fig. 9. Effect of temperature on porosity, surface oxy functional groups and unpyrolyzed organic mater of the biochar [61].

#### 4. Applications

This session presents applications of biochar, activated carbon, and CNM as individual and in comparisons. For the comparison study, their different performances are discussed based on chemical and physical characteristics provided in the same references or predicted based on data of characteristics in session 4 as long as possible. Biochar can be applied as catalyst, energy storage such as electrode, soil amandement to increase soil fertility and quality, adsorbent of organic and inorganic contaminant in the soil and aquatic environment, and composting to enhance microbial population and minerals [38]. Biochar in compost with sewage sludge decreased the abundance of *Escherichia coli* and *Salmonella* ssp [64]. The biochars made from woody or leafy material have high porosity and improve water content in the soils [65]. Biochar reduce greenhouse gas emissions from the soil and remove pollutants of heavy metals, pigments, pharmaceuticals, aromatic and polyaromatic hydrocarbons, also pathogenic organism from aqueous solutions [39].

Activated carbon widely is used as adsorbent, catalyst and catalyst supports. The matchness of adsorbent pore size and adsorbate size determines effectivity of adsorption [23]. Carboxyl, carbonyl, lactone, phenol and quinone are the main functional groups of the activated carbon which are responsible to adsorb pollutants [66]. Activated carbons (ACs) are widely also applied in medical, electronic and environment products [6].

CNS have developed tremendous interest in the world because of their remarkable structural, electrical, optical, thermal, mechanical and chemical properties. By designing novel arrangements such as ribbon, hybrid, polymer, dopping, and hetero-structures, the carbon nanomaterials were moved by researches of various disciplines [67].

CNS such as CNT and graphene were used as Pt and platinum oxide nanoparticles matrix to control their size, distribution and amount of the deposited particles. As matrix, CNT provides additional advantages, such as a conductive characteristics, large surface area, fast response time, high electron transfer rate, easy immobilization [68]. CNTs have attractive electronic and optical properties, small size, good biocompatibility, good surface function, and high reactivity. Therefore, CNTs can be widely used in the fields of energy, biomedicine, electronics, photoelectricity, analysis, and catalysis [69].

Compared to activated carbon, biochar makes the anaerobic metabolism of the biofilm higher and has a longer lifetime than GACs in bioelectrochemical systems. Therefore, the wood-derived biochar has been studied to replace GACs in contaminant removal applications [37]. Increasing applications of biochar are determined by its characteristics such as surface

area, pore volume, pore size, pH, cation exchange capacity (CEC), electrical conductivity (EC) and surface functional groups, as well as its sustainable, easy and low cost production process [39].

Comparison of the three materials in their applications as adsorbents have been conducted by some research. For example, removal of Pb(II) cations by CNT, AC (activator of H<sub>3</sub>PO<sub>4</sub>) and AC (activator of KOH). After adsorption process in various times (1, 24, and 72 h), the adsorption effectivity showed in sequence of AC (KOH) > AC (H<sub>3</sub>PO<sub>4</sub>) > CNT. Physically, data of specific surface area (*S*<sub>BET</sub>) and pore volume characterizations shows in the same sequences. XPS characterization reported that chemically AC (H<sub>3</sub>PO<sub>4</sub>) and CNT had surface functional groups of C-O and O-C=O in similar intensities [70]. The Pb(II) cation is Lewis acid and those oxygenated functional groups are the Lewis base which attracted the Pb(II) cations in the adsorption process. Therefore, the adsorption difference is probably more affected by difference of the physical properties.

The other comparison is about adsorption of <sup>14</sup>C-catechol by various carbons (biochar, AC, SWCNT, and MWCNT) and soil. The sequence of the adsorbed catechol as follows: SWCNT > MWCNT > AC > biochar > soil. The other experiment, the extracted microbe from the fresh soil by addition of various carbons (0,2 mg/Kg) after incubation at 25°C in the dark for 61 days were in sequence: control = biochar > MWCNT > SWCNT > AC. It means that growth of the microbe in the soil is not affected by biochar but reduced by the other carbons' adsorptions. No characterizations of functional groups, surface area, and pore volume were reported to discuss [71]. However, based on characteristics of AC and CNT in Table 4 it can be predicted that physical properties including specific surface area and pore volume may determine the sequence.

Comparison among the activated carbons with different pyrolysis methods and different activators affect the adsorption capacity of dyes and metal cation, as listed in Table 5. The pyrolysis methods include hydrothermal (HTC) and slow pyrolysis (SP). The used activators are H<sub>3</sub>PO<sub>4</sub>, CO<sub>2</sub>, and KOH. Table 5 confirms that the highest adsorption capacity of the both dyes was achieved by AC (HTC H<sub>3</sub>PO<sub>4</sub>) due to the lowest AC pH (most acid). Oppositely, the largest one of Zn<sup>2+</sup> was obtained by AC (SP CO<sub>2</sub>) due to the highest AC pH (most base). It means that dyes and Zn<sup>2+</sup> prefer the AC surfaces with the most acid groups and the least acid groups, respectively. The kind of the oxy groups role in the adsorption capacity can be determined by Pierson correlation coefficient as presented in Table 6. Based on Table 6 the phenolic groups have the most role for adsorption of dyes, whereas the lactonic has the most role for Zn<sup>2+</sup> adsorption. The imagination of interaction is given in Figure 10.

**Table 5: Adsorption capacity of dyes and metal cation by AC with different pyrolysis method and activator (%)**

AC	Methylen blue	Acid orange II	Zn <sup>2+</sup>	AC pH	References
HTC H <sub>3</sub> PO <sub>4</sub>	92	95	7	3.9	[53]
HTC CO <sub>2</sub>	55	47	13	5.4	[53]
HTC KOH	80	50	61	6.2	[53]
SP H <sub>3</sub> PO <sub>4</sub>	62	52	5	4.2	[53]
SP CO <sub>2</sub>	54	52	98	9.5	[53]
SP KOH	91	67	88	7.2	[53]

**Table 6: Pierson correlation coefficient of acidic surface groups and adsorption capacity**

Oxy groups	Methylene blue	Acid orange II	Zn <sup>2+</sup>	References
Carboxyl	0.57	0.47	-0.48	[53]
Lactone	0.63	0.11	0.36*	[53]
Phenol	0.8*	0.7*	-0.56	[53]
Total acidity	0.8	0.48	-0.15	[53]

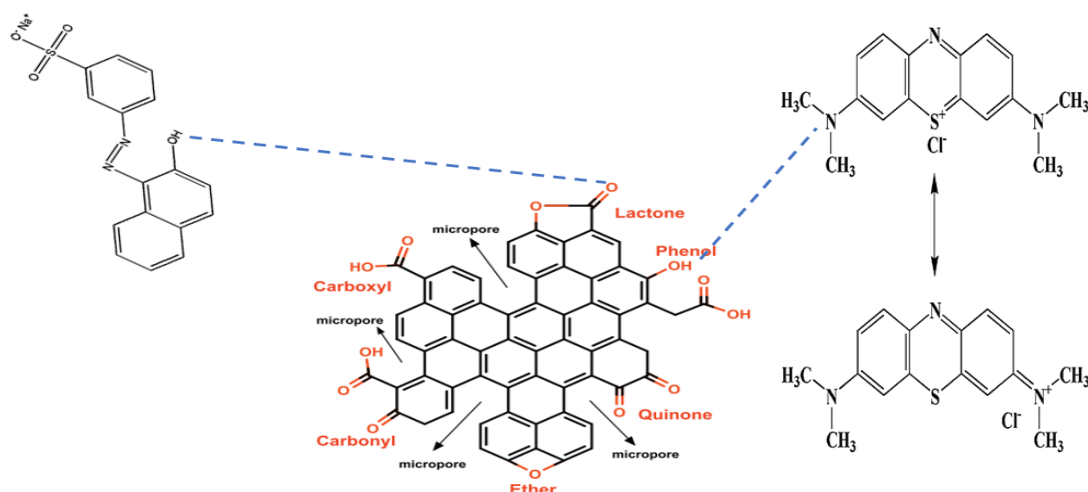


**Fig. 10. Chemical interactions of methylene blue – phenolic group(AC) and acid orange II – lactonic group (AC)**  
[58, 72,73]

Adsorptions of multi component solutions by different adsorbents such as biochar and activated magnetic biochar are presented in Figure 11. The multi components include Cu(II)-sulfamethoxazole and Cu(II)-17 $\beta$ -estradiol for adsorption of rice straw biochar and of rice straw activated magnetic biochar, respectively. Figure 11 confirms that the activated magnetic biochar has higher maximum adsorption than the biochar.

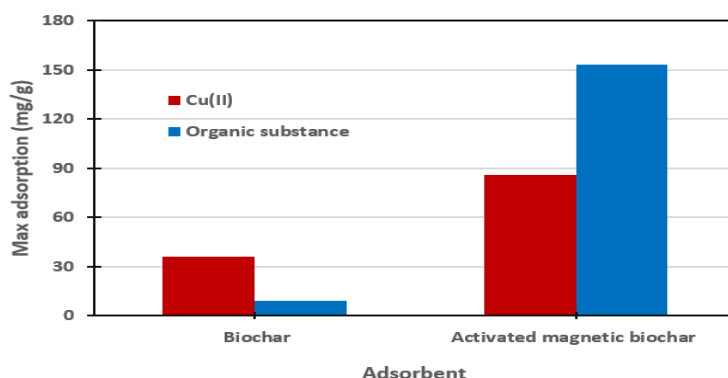


Fig. 11. Maximum adsorption of Cu(II) cations and organic substances by different rice straw adsorbents [40]

Possible adsorption mechanisms of inorganic ions and organic compounds by both adsorbents were designed in Figure 12 to explain the difference of adsorption. The possibilities of mechanisms include adsorption of organic molecules then followed by adsorption of metal cations, adsorption of the metal cations then followed by the organic molecules, and adsorption of the cation – organic molecules as the complex molecules [40]. The formation of the complex compound before adsorption or sequent adsorption of metal cations and organic molecules are supported by attraction force of Cu(II) as Lewis acid and the organic molecules as Lewis bases. Based on general comparison properties of the biochar to of the activated carbon, higher adsorption of both Cu(II) cation and the organic molecules by the activated carbon than the biochar might be caused by its higher surface area and pore volume and richer oxygenated functional groups due to activation treatment.

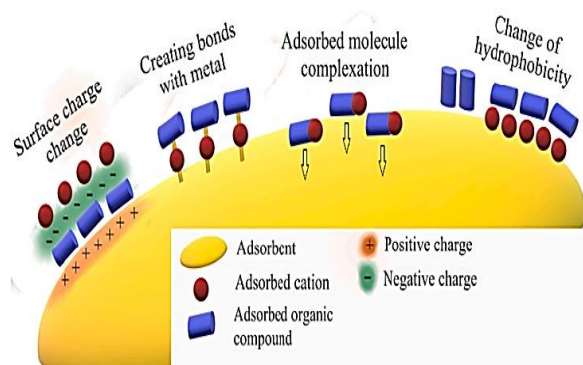


Fig. 12. Possible mechanism of metal cation and organic substance adsorption on activated carbon and biochar surfaces [40]

Comparison of Pb(II) adsorption by biochar VS biochar-CNT composite was reported in Table 7. The Langmuir isotherm model in Table 7 suggests that the interactions between Pb(II) and the sorbents might be mainly the mono-layer adsorption. The maximum adsorption amount of Pb(II) on CS-CNT was significantly higher than that on CS, indicating that CNT can enhance the Pb(II) sorption ability of biochar due to the improved surface area and pore volume. The characterization by FTIR spectrometry confirm similar functional groups of the adsorbent's surfaces including types and intensities. The functional groups which may have the role in interaction with Pb(II) Lewis acid are C=O, -OH, COO-, and C-O Lewis bases can be designed as adsorption mechanism in Figure 13.

Table 7: Adsorption of Pb(II) cations by biochar and biochar-CNT composite

Sample	SSA	Pore volume	Langmuir model		References
			$q_m(308^\circ\text{C})$	$R^2$	
Pristine biochar	193.52	0.077	1294.44	0.998	[74]
Biochar-CNT	231.6	0.09	1334.65	0.999	[74]



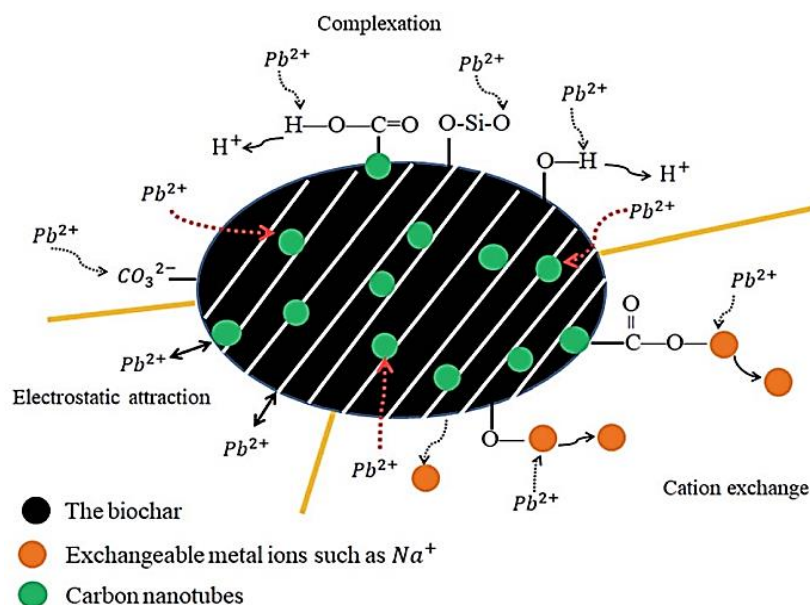


**Fig. 13. Proposed adsorption mechanism of Pb(II) on biochar-CNT [74]**

Comparison of SDS adsorption by activated carbon and biochar is listed in Table 8. The Langmuir model in Table 8 reported higher maximum adsorption of SDS by activated carbon than biochar. Physically, it can be related to much higher surface area of the activated carbon than of the biochar. The chemical interactions of the SDS and the adsorbents were explained based on the functional groups which were identified from their FTIR spectra. Prior to SDS adsorption, the adsorbents exhibited oxygen-containing functional groups, including hydroxyl ( $-O-H$ ) and carbonyl ( $C=O$ ) stretching of carboxylic, ester, ketone and aldehyde groups. After SDS adsorption, the FTIR spectra absorption intensity difference were observed. Therefore, chemically the adsorption may be controlled by interaction between negative charges of the deprotonated hydroxyl of the adsorbents and the positive charges of SDS heads. The additional weak chemical interaction may be between hydrophobic aliphatic hydrocarbon of the adsorbent and hydrophobic chains of the SDS surfactant. Those chemical interactions are designed in Figure 14.

**Table 8: Sodium dodecyl sulphate (SDS) adsorption by activated carbon and biochar**

Sample	SSA (m <sup>2</sup> /g )	Langmuir model		References
		q <sub>max</sub> (mg/g)	R <sup>2</sup>	
Activated carbon	1500–3000	80.65	0.963	[75]
Biochar	300	45.87	0.955	[75]

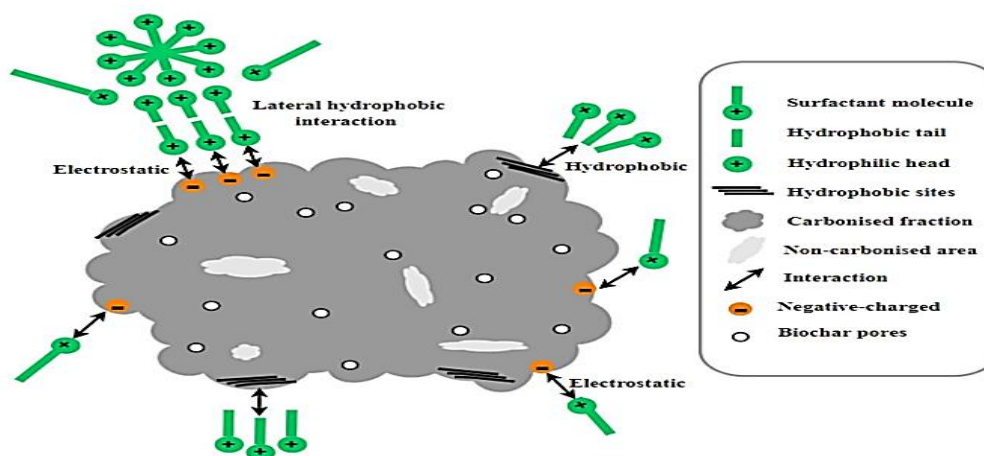


**Fig. 14. Surfactant adsorption mechanism [75].**

Adsorptions of different metal cations by 4 different adsorbents are presented in Table 9. Generally, adsorption data in Table 9 shows that adsorption of metal cations by activated carbon is higher than CNT, but less than both oxidized CNT and NaOCl-modified CNT. No data of surface area and functional groups type of the carbon based on characterization, but based on oxidation and NaOCl modification treatments, the main mechanism is probably due to the chemical interactions of the metal ions and surface functional groups of CNTs, including surface anion OCl<sup>-</sup> from modification and oxy functional groups which were created by oxidation reaction.

**Table 9: Metal cation adsorptions by activated carbon, CNT, oxidized CNT and modified CNT**

Adsorbates	Adsorbents	Q (mg/g)	Adsorption condition	References
Cu <sup>2+</sup>	As-produced CNTs	8.25	pH 6, 300K	[67]
	NaOCl-modified CNTs	47.4	pH 6, 300K	[67]
	Activated carbon	19.5	pH 6, 300K	[67]
Ni <sup>2+</sup>	NaOCl-modified MWCNTs	38.5	pH 5, 298K	[67]
	Granule activated carbon	2.88	pH 5, 298K	[67]
Pb <sup>2+</sup>	Oxidized MWCNTs	97.1	pH 5, 298K	[67]
	AC/ F-400	30.1	pH 5, 298K	[67]
Cd <sup>2+</sup>	Oxidized MWCNTs	10.9	pH 5, 298K	[67]
	AC/ F-400	8	pH 5, 298K	[67]

## 5. Synthesis methods

Combustion and pyrolysis are same thermochemical conversion techniques which employ heat to break down the organic material bonds with different concepts. Chemically, combustion is the thermal oxidation reaction in oxygen presence to produce CO<sub>2</sub> and H<sub>2</sub>O (hot flue gas) with ash as the side product. Pyrolysis products are solid (char), liquid (tar, water) and non-condensable gases (H<sub>2</sub>, CO, CO<sub>2</sub> and CH<sub>4</sub>) [76].

### Synthesis method of biochar

The biochar fraction is determined by pyrolysis types, including slow pyrolysis, intermediate pyrolysis, fast pyrolysis gives biochar product of 35%, 25%, and 12 %, respectively. Those pyrolysis methods can have same temperature range (450 – 500°C) but exactly different residence time, including hours to days, 10-20 s, and < 2 s, respectively. The slow pyrolysis by torrefaction, hydrothermal, and microwave assistance techniques achieve the biochar product of 75%, 35%, and about 30% respectively.

In pyrolysis process, the lignocellulosic substances of biomass (hemicellulose, cellulose, and lignin) experience the decomposition reactions in the different temperatures, such as 200-300°C, 400°C and 500°C, respectively [38].

For example, dried spent coffee grounds (SCG) was used to produce biochar by slow pyrolysis at three different temperatures: 300, 450, and 600 °C. A heating rate of 5 °C.min<sup>-1</sup> was applied with a residence time at the set temperature of 30 min. No explanation about nitrogen gas stream. There was decreasing of yield, bulk density, O/C ratio of biochar, but increasing of electric conductivity, pH, oil holding capacity, and metal content (K, Fe, Cu, Mn) by increasing temperature. [2].

Coffee-ground biochar (CGB) was synthesized from spent coffee grounds (SCG) through slow pyrolysis experiments to 500 °C for 1 h under nitrogen gas streaming. The CGB was modified with TiO<sub>2</sub> using a sol-gel method and labelled as CGBT. The CGBT has lower crystal size, larger S<sub>BET</sub> and pore volume and smaller pore size, and smaller band gap than TiO<sub>2</sub>. Photocatalytic degradation of pentachlorophenol (PCP) by CGBT has higher k (11.4 X), higher % degradation (3,7 X), destruction rate (14 X) than by CGB [3].

Tea waste was torrefied in a Thermogravimetric analyzer LECO TGA 701 at a rate of 10 °C. min<sup>-1</sup> at 250, 300, 350, 450, 550°C. Analysis of element with the Elemental analyzer shows that there are increasing of carbon and ash but decreasing of hydrogen and oxygen by increasing of temperature. The phytotoxicity test show that untorrefied tea and torrefied at 250 °C are toxic and unsuitable for soil application. Heat treatment at higher temperatures decomposes substances that have a negative effect on germination. The sample treated at 350 °C showed the highest germination index for all grinding fraction sizes. [4]. The waste tea was pyrolysed at 500 °C for 2 h in tube furnace under a N<sub>2</sub> atmosphere, then calcined by an activation gas of steam and nitrogen flow at 700°C for 45 min. The activated biochar (HC) was modified by NH<sub>4</sub>Cl solution by magnetic stirring and then ultrasonic. The modified biochar has higher both S<sub>BET</sub> and V<sub>p</sub> (141.53 m<sup>2</sup>/g ; 0,084 cm<sup>3</sup>/g) than activated biochar (122.53 m<sup>2</sup>/g; 0.055 cm<sup>3</sup>/g). It has Hg removal capacity of 1079 µg/g [5].

### Synthesis method of activated carbon

Activated carbon are produced in 2 steps including carbonization and activation [6,23]. Carbonization is pyrolysis reaction of the raw materials [23]. Carbonization converts biomass to carbonaceous structure and activation forms the carbon pores physically or chemically. Both processes increase the oxygenated functional group and porosity structure on carbon surface and consequently improve water adsorption [6]. Activation can also enlarge fine pores besides create new pores after carbonization. Activation is performed physically using steam (H<sub>2</sub>O) or CO<sub>2</sub> gas at high temperatures (800 – 1300 °C). The chemical activation uses acidic agents (HCl, H<sub>3</sub>PO<sub>4</sub>, H<sub>2</sub>SO<sub>4</sub>, ZnCl<sub>2</sub>) or basic reagents (KOH, NaOH, etc). However carbonization and activation processes can be carried out simultaneously by thermal decomposition of the chemical activator impregnated precursors [23].

AC and biochar are samely produced from pyrolysis of biomass under oxygen devoid conditions. The major difference of biochar and AC is other production process condition. AC, is produced at higher temperatures than biochar. Biochar is produced at around 400°C or less, while AC is produced at about 700 to 900°C. Activation step is compulsory either before or after carbonization for AC, but not compulsory for biochar. In both carbon materials, the thermal treatment stabilizes the biomass core-structure by improving the physicochemical properties of the materials [77].

Dried fresh coffee grounds and dried fresh tea leaves were carbonized at 560 °C for 4h and then was activated with nitric acid (HNO<sub>3</sub>) and then by 1 molar of potassium hydroxide (KOH). Washing with DI water and drying at 100 °C was conducted every after activation process. The ACs based on the coffee grounds and tea leaves have the codes of CA and TA, respectively. There is similarity of FTIR spectra patterns, including kind of peaks at ~3420 cm<sup>-1</sup> (OH), at ~1583 cm<sup>-1</sup> (C=C) and at ~1384 cm<sup>-1</sup> (C-O) except CA has sharper peak than TA. Adsorption capacity of iron (II) by TA was higher than CA. The Fe(II) cation concentration in the filtrate after filtration by TA and CA is 0.13 and 0.2 mg/L, compared to unfiltered water (0.3 mg/L) [6].

Potassium hydroxide (KOH) and dried spent coffee grounds (SCG) were mixed in mass ratios of 1:1 and 2:1 (KOH: SCG), weighed in crucibles and placed in the tubular furnace with nitrogen gas flow and the temperature was set to 400 or 600°C for 1 or 2 h, then washed with distilled water until a neutral pH to remove the KOH residual, then dried at 105 °C for ~12 h [7].

The dried waste tea (WT) was pyrolyzed using KOH (KWT) and NaOH (NWT) activators at impregnation ratio of activating agent: biomass 1:1 and the activation temperature of 600 °C. Small quantities of SiO<sub>2</sub> nanoparticles (2.5, 5, and 7.5%) were physically added to AC by hand dry-mixing method and designated as K.WT.Sx (x is the weight percentage of silica). There was increasing of S<sub>BET</sub> (59.15 to 453.18 m<sup>2</sup>/g) and V<sub>BJH</sub> (0.03 to 0.307 cm<sup>3</sup>/g) for sequence of WT < NWT < KWT < KWTS2.5. The decreasing is available for more silica addition treatment. The FTIR spectra showed weaker bands at 3391-3404, 1557-1647, 997-1052 cm<sup>-1</sup> related to the -OH, aromatic C=C, and C-O functional groups respectively for sequence of WT > KWT > NWT. There was increasing of carbon dioxide capture capacity by same sequence of specific surface area and pore volume [8].

Waste tea were carbonized at room temperature by addition of piranha solution (75 mL H<sub>2</sub>SO<sub>4</sub> 98 %-25 mL H<sub>2</sub>O<sub>2</sub> 30 %) at ratio of 2:5. The fast (10-15 min) and exothermic reactions complete carbonization of the waste tea by formation of CO<sub>2</sub> gas and hot steam vapor (H<sub>2</sub>O). The XRD pattern shows a very broad (002) reflection with d<sub>002</sub> = 4.5 Å, larger than crystalline graphite with d<sub>002</sub> = 3.4 Å indicating amorph, highly disordered carbon. Raman spectroscopy shows intensity ratio ID/IG = 0.49, indicative of amorphous carbon. XPS spectra shows ratio of sp<sup>2</sup>/sp<sup>3</sup> carbons (58.7 %), the functional groups contents of C-O (23.5 %), C=O (9.5 %) and O-C=O (6.8 %). SEM and TEM confirms the presence of large nanosheets. AFM confirms that the nanosheets consist of both thin sheets with thickness 1-2.5 nm and thick sheets with thickness 2.5-35 nm. The waste tea-derived carbon reacts hypergolically with fuming nitric acid (HNO<sub>3</sub>) at ambient conditions probably due to large space between graphene layers [9].

### Synthesis method of CNM or CNS

Carbon nanomaterial can be produced from AC in 2 ways, including by physical and chemical treatments. For the physical way, the AC particle size is directly reduced to achieve 1-100 nm, including mixing by mixer, blending by blender, sonication by sonicator, and stirring by stirrer. Among those all mixer is the best technique. By these technique, the structure of CNM will be same (turbostratics) with the AC [10,41]. The CNM synthesis route is described in Figure 15. For the chemical way, the AC was pyrolyzed again using other organic precursor and chemical activator. For example, CNT was prepared by dry pyrolysis of activated carbon, melamine, and iron (III) oxalate mixture at 600 and 900°C sequently. The structure of CNT was proved virtually by SEM and TEM [78]. CNM was also prepared from biochar by ball milling of the biochar. The product was called as nano-biochar [79].

CNM can be also prepared directly from biomass with activator such as preparation of AC but involving mechanical treatment such as ball milling of precursor before pyrolysis. For example, waste coffee ground was grinded by ball milling at 1000 rpm then carbonized together with a chemical activator of KOH at 700°C under nitrogen flow. The product was named nano porous carbon (NPC). The product was mixed with CNT and grinded by ball milling again at 1000 rpm. The scheme of preparation is given in Figure 16. The NPC has S(BET) of 706.5 m<sup>2</sup>/g and V<sub>p</sub> 0.23 cm<sup>3</sup>/g. The mixture of NPC and CNT (3%) increase both specific surface area and pore volume to 1158 m<sup>2</sup>/g and 0.34 cm<sup>3</sup>/g [13]. The other example, carbon nanoflake was prepared by pyrolysis of ferrocene (Fe(C<sub>5</sub>H<sub>5</sub>)<sub>2</sub>) and tea waste mixture in tubular furnace at 900°C for 1 h under argon streaming. No additional treatment to conditionize the solid particle size. FE-SEM confirmed the width range of these nanoflakes from 15- 55 nm and few of 65-75 nm. Raman spectra of carbon nanoflakes show ratio of relative intensity (D/G = 1.24), suggesting the low disorder. The oxy functional group of the surface is C-O and S=O [1].

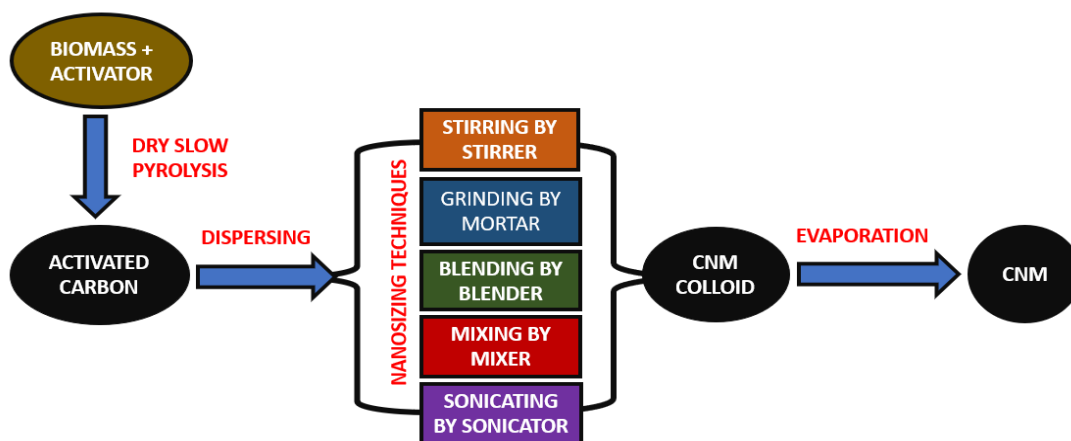


Fig. 15. Scheme of CNM synthesis route using various nanosizing techniques [10-12,43]

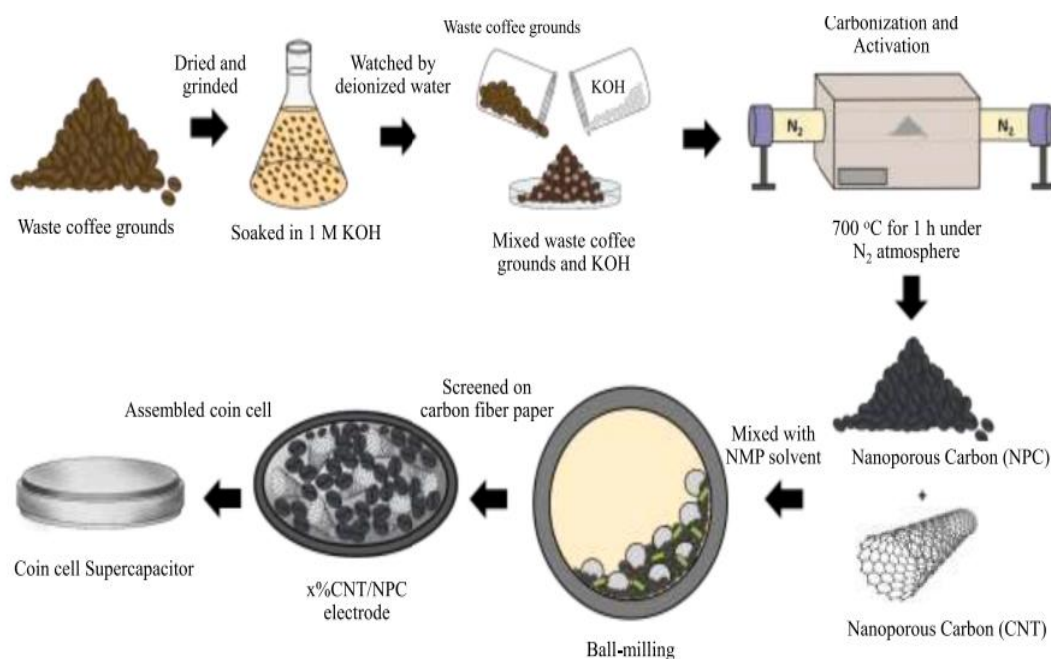


Fig. 16. Scheme of NPC preparation from waste coffee ground [13]

## 6. Conclusions

Biochar, activated carbon, and CNM are 3 physically and chemically different materials but have same carbon atoms as the main content. Physically, they have different surface area and pore volume. Chemically, they have different chemical structures due to their different preparation methods. Those materials can be prepared from coffee and tea due to their lignocellulosic substances, including cellulose, lignin, and hemicellulose.

## 7. Conflicts of interest

“There are no conflicts to declare”.

## 8. References

- [1]. Mahal, E. and Al-Mutlaq, S., Bio-Based carbon nanomaterials synthesis from waste tea, *Eurasian Chemical Communications*, 5(3), 264 – 270, (2023). <https://doi.org/10.22034/ecc.2023.366295.1541>
- [2]. Al-Awadhi, Y.M., Pradhan, S., McKay, G., Al-Ansari, T., and Mackey, H.R., Coffee Waste Biochar: a Widely Available and Low-cost Biomass for Producing Carbonaceous Water Treatment Adsorbents, *Chemical Engineering Transactions*, 92, 319 – 324, (2022). <https://doi.org/10.3303/CET2292054>
- [3]. Changotra, R., Rajput, H., Yang, J., Dasog, M., and He, Q.S., Spent-coffee grounds-derived biochar-supported heterogeneous photocatalyst: a performance evaluation and mechanistic approach for the degradation of pentachlorophenol, *RSC Sustainability*, 1, 1484 – 1496, (2023). <https://doi.org/10.1039/D3SU00153A>
- [4]. Tunklová, B., Jeníček, L., Maláček, J., Neškudla, M., Velebil, J., and Hnilíčka, F., Properties of Biochar Derived from Tea Waste as an Alternative Fuel and Its Effect on Phytotoxicity of Seed Germination for Soil Applications, *Materials*, 15(24), 8709, (2022). <https://doi.org/10.3390/ma15248709>
- [5]. Shen, B., Tian, L., Li, F., Zhang, X., Xu, H., and Singh, S., Elemental mercury removal by the modified bio-char from waste tea, *Fuel*, 187, 189 – 196, (2017). <https://doi.org/10.1016/j.fuel.2016.09.059>
- [6]. Dulyaseree, P., Mahasae, F., Hayeekueji, N., and Yordsri, V., Comparison of Efficiency of Activated Carbon Between Coffee Grounds, Soybean Straw and Tea Leaves, *Journal of Physics: Conference Series*, 2049, 012055, (2021). <https://doi.org/10.1088/1742-6596/2049/1/012055>
- [7]. Campbell, R., Xiao, B., and Mangwandi, C., Production of activated carbon from spent coffee grounds (SCG) for removal of hexavalent chromium from synthetic wastewater solutions, *Journal of Environmental Management*, 366, 121682, (2024). <https://doi.org/10.1016/j.jenvman.2024.121682>
- [8]. Tahmasebpour, M., Iranvandi, M., Heidari, M., Azimi, B., and Pevida, C., Development of novel waste tea-derived activated carbon promoted with SiO<sub>2</sub> nanoparticles as highly robust and easily fluidizable sorbent for low-temperature CO<sub>2</sub> capture, *Journal of Environmental Chemical Engineering*, 11(5), 110437, (2023). <https://doi.org/10.1016/j.jece.2023.110437>
- [9]. Asimakopoulos, G., Moschovas, D., Avgeropoulos, A., Bourlinos, A.B., Tantis, I., Sedajová, V., Tomanec, O., Salmas, C.E., Gournis, D., and Karakassides, M.A., From Waste Tea to Carbon Rocket Fuels through a Piranha Solution-Mediated Carbonization Treatment, *Journal of Nanotechnology Research*, 4, 31 – 44, (2022).



- <https://www.fortunejournals.com/articles/from-waste-tea-to-carbon-rocket-fuels-through-a-piranha-solution-mediated-carbonization-treatment.html>
- [10]. Setianingsih, T., Purwonugroho, D., and Prananto, Y.P., Sintesis CNS dari Berbagai Tepung dengan Microwave, Laporan Penelitian DPP-SPP, Brawijaya University, Malang, (2021).
  - [11]. Setianingsih, T. and Darjito, Sintesis Komposit Nano Fe(III)-Doped Kaolin – ZnFe<sub>2</sub>O<sub>4</sub>/CNS dari Serbuk Kopi dan The dengan Metode Hydrothermal dan Microwave, Laporan Penelitian Dasar I, Brawijaya University, Malang, (2023a).
  - [12]. Setianingsih, T., Darjito, and Kamulyan, B., Optimasi Pada Sintesis Komposit Fe(III) Dopped Kaolin – ZnFe<sub>2</sub>O<sub>4</sub> / CNS dari Serbuk Kopi dan Teh untuk Meminimasi Pencemaran Tanah Sawah oleh Pestisida, Laporan Hibah Doktor Lektor Kepala, Brawijaya University, Malang, (2023b).
  - [13]. Poochai, C., Srihaow, A., Lohitkarn, J., Kongthong, T., Tuantranont, S., Tuantranont, S., Primpray, V., Maeboonruan, N., Wisitorsa, A., and Sriprachuabwong, C., Waste coffee grounds derived nanoporous carbon incorporated with carbon nanotubes composites for electrochemical double-layer capacitors in organic electrolyte, *Journal of Energy Storage*, 43, 103169, (2021). <https://doi.org/10.1016/j.est.2021.103169>
  - [14]. Setianingsih, T., Masruri, and Ismuyanto, B., Biochar dan Fungsionalisasi Biochar, UB Press, Malang, (2018). [https://books.google.co.id/books/about/Biochar\\_dan\\_Fungsionalisasi\\_Biochar.html?id=snLcDwAAQBAJ&redir\\_esc=y](https://books.google.co.id/books/about/Biochar_dan_Fungsionalisasi_Biochar.html?id=snLcDwAAQBAJ&redir_esc=y)
  - [15]. Noprianti, N.S.A., Hamdi, and Sudiar, N.Y., Analisis Pemanfaatan Biobriket Dari Limbah Kulit Kopi Sebagai Basis Pengembangan Energi Terbarukan, *Journal of Applied Mechanical Engineering and Renewable Energy*, 4(2), 1 – 9, (2024). <https://journal.isas.or.id/index.php/JAMERE/article/view/837/289>
  - [16]. Warsito, K., Asmaq, N., Irawan, I., Purba, N.S., and Heinze, J., Potential of Utilizing Arabika Coffee Dregs (*Coffea Arabica* L.) as Biochar for Increasing Fertility of Plant Media, *The International Conference on Education, Social, Sciences and Technology (ICESST)*, 2(2), 359 – 367, (2023). <https://ijconf.org/index.php/icesst/article/view/332>
  - [17]. Yu, D., Zeng, S., Wu, Y., Niu, J., Tian, H., Yao, Z., and Wan, X., Removal of tetracycline in the water by a kind of S/N co-doped tea residue biochar, *Journal of Environmental Management*, 365, 121601, (2024). <https://doi.org/10.1016/j.jenvman.2024.121601>
  - [18]. Wankhade, A.A. and Ganvir, V.N., Preparation of Low Cost Activated Carbon from Tea Waste using Sulphuric Acid as Activating Agent, *International Research Journal of Environment Sciences*, 2(4), 53 – 55, (2013). <https://www.isca.in/IJENS/Archive/v2/i4/13.ISCA-IRJEvS-2013-094.php>
  - [19]. Al-Hazmi, G.H., Saad, H.A., Refat, M.S., and Adam, A.M.A., Fe<sub>3</sub>O<sub>4</sub>-Carbon-Based Composite Derived from the Charge-Transfer Reaction Using Waste Tea Leaves as the Carbon Precursor for Enhanced Removing of Azocarmine G2, Methyl Violet 2B, Eosin B, and Toluidine Blue from Aqueous Solution, *Crystals*, 12(10), 1355, (2022). <https://doi.org/10.3390/cryst12101355>
  - [20]. Menon, R., Singh, J., Doshi, V., and Lim, X.Y., Investigation on Spent Tea Leaves Derived Activated Carbon For CO<sub>2</sub> Adsorption, *Journal of Engineering Science and Technology*, Special Issue April, 50 – 61, (2015).
  - [21]. Kalita, R.M., Das, A.K., and Nath, A.J., Allometric equations for estimating above- and belowground biomass in Tea (*Camellia sinensis* (L.) O. Kuntze) agroforestry system of Barak Valley, Assam, northeast India, *Biomass and Bioenergy*, 83, 42 – 49, (2015). <https://doi.org/10.1016/j.biombioe.2015.08.017>
  - [22]. Rafidah, H.S., Prasetia, H., and Saefumillah, A., Adsorption Study of Methylene Blue and Methyl Red on Activated Carbon from Silver Composite Using the Extract of Spent Coffee Grounds, *Jurnal Sains Materi Indonesia*, 25(2), 77 – 84, (2024). <https://doi.org/10.55981/jsmi.2024.924>
  - [23]. Boomannuayvitaya, V., Chaiya, C., and Tanthapanichakoon, W., The preparation and Characterization of Activated carbon from Coffee Residue, *Journal of Chemical Engineering of Japan*, 37(12), 1504 – 1512, (2004). <https://doi.org/10.1252/jcej.37.1504>
  - [24]. Lozano-Pérez, A.S. and Guerrero-Fajardo, C.A. Liquid Hot Water (LHW) and Hydrothermal Carbonization (HTC) of Coffee Berry Waste: Kinetics, Catalysis, and Optimization for the Synthesis of Platform Chemicals, *Sustainability*, 16(7), 2854, (2024). <https://doi.org/10.3390/su16072854>
  - [25]. Gul, E., Al Bkour Alrawashdeh, K., Masek, O., Skreiberg, Ø., Corona, A., Zampil, M., Wang, L., Samaras, P., Yang, Q., Zhou, H., Bartocci, P., and Fantozzi, F., Production and use of biochar from lignin and lignin-rich residues (such as digestate and olive stones) for wastewater treatment, *Journal of Analytical and Applied Pyrolysis*, 158, 105263, (2021). <https://doi.org/10.1016/j.jaap.2021.105263>
  - [26]. Robertson, D., Nousiainen, P., Pitkänen, L., Schlapp-Hackl, I., Rusakov, D., and Hummel, M., Carbonisation of lignin in the presence of a eutectic salt mixture: Identifying the lignin properties that govern the characteristics of the resulting carbon material, *Journal of Analytical and Applied Pyrolysis*, 183, 106811, (2024). <https://doi.org/10.1016/j.jaap.2024.106811>
  - [27]. Widiyastuti, W., Rois, M.F., Setyawan, H., Machmudah, S., and Anggoro, D., Carbonization of Lignin Extracted from Liquid Waste of Coconut Coir Delignification, *Indones. J. Chem.*, 20(4), 842 – 849, (2020). <https://doi.org/10.22146/ijc.46484>
  - [28]. Xu, X., Pan, H., Shen, Q., Tan, X., Ding, D., and Wang, Y., Preparation and Application of lignin carbon fiber, *Journal of Physics: Conference Series*, 1790, 012071, (2021). <https://doi.org/10.1088/1742-6596/1790/1/012071>
  - [29]. Hwang, U.T., Bae, J., Lee, T., Hwang, S.Y., Kim, J.C., Park, J., Choi, I.G., Kwak, H.W., Hwang, S.W., and Yeo, H., Analysis of Carbonization Behavior of Hydrochar Produced by Hydrothermal Carbonization of Lignin and Development of a Prediction Model for Carbonization Degree Using Near-Infrared Spectroscopy, *J. Korean Wood Sci. Technol.*, 49(3), 213 – 225, (2021). <https://doi.org/10.5658/WOOD.2021.49.3.213>
  - [30]. Burra, K.G., Daristotle, N., and Gupta, A.K., Carbonization of Cellulose in Supercritical CO<sub>2</sub> for Value-Added Carbon, *Journal of Energy Resources Technology*, 143, 1 – 10, (2021). <https://doi.org/10.1115/1.4050634>
  - [31]. Paksung, N., Pfersich, J., Arauzo, P.J., Jung, D., and Kruse, A., Structural Effects of Cellulose on Hydrolysis and Carbonization Behavior during Hydrothermal Treatment, *ACS Omega*, 5, 12210 – 12223, (2020). <https://doi.org/10.1021/acsomega.0c00737>

- [32]. Sermiyagina, E., Murashko, K., Nevstrueva, D., Pihlajamäki, A., and Vakkilainen, E., Conversion of cellulose to activated carbons for high- performance supercapacitors, *Agronomy Research*, 18(3), 2197 – 2210, (2020). <https://doi.org/10.15159/AR.20.163>
- [33]. Yu, S., Dong, X., Zhao, P., Luo, Z., Sun, Z., Yang, X., Li, Q., Wang, L., Zhang, Y., and Zhou, H., Decoupled temperature and pressure hydrothermal synthesis of carbon sub-micron spheres from cellulose, *Nature Communications*, 13, 3616, (2022). <https://doi.org/10.1038/s41467-022-31352-x>
- [34]. Wei, Y., Chen, W., Liu, C., Wang, H., Facial Synthesis of Adsorbent from Hemicelluloses for Cr(VI) Adsorption, *Molecules*, 26(5), 1443, (2021). <https://doi.org/10.3390/molecules26051443>
- [35]. Zhu, L. and Zhong, Z., Effects of cellulose, hemicellulose and lignin on biomass pyrolysis kinetics, *Korean J. Chem. Eng.*, 37(10), 1660 – 1668 (2020). <https://doi.org/10.1007/s11814-020-0553-y>
- [36]. Chen, D., Cen, K., Zhuang, X., Gan, Z., Zhou, J., Zhang, Y., and Zhang, H., Insight into biomass pyrolysis mechanism based on cellulose, hemicellulose, and lignin: Evolution of volatiles and kinetics, elucidation of reaction pathways, and characterization of gas, biochar and bio-oil, *Combustion and Flame*, 242, 112142, (2022). <https://doi.org/10.1016/j.combustflame.2022.112142>
- [37]. Van Limbergen, T., Roegiers, I.H., Bonn , R., Mare, F., Haeldermans, T., Joos, B., Nouwen, O., Manca, J.V., Vangronsveld, J., and Thijs, S., Characterisation of Two Wood-Waste and Coffee Bean Husk Biochars for the Removal of Micropollutants from Water, *Frontiers in Environmental Science*, 10, 814267, (2022). <https://doi.org/10.3389/fenvs.2022.814267>
- [38]. Amalina, F., Razak, A.S.A., Krishnan, S., Sulaiman, H., Zularisam, A.W., and Nasrullah, M., Biochar production techniques utilizing biomass waste-derived materials and environmental applications – A review, *Journal of Hazardous Materials Advances*, 7, 100134, (2022). <https://doi.org/10.1016/j.hazadv.2022.100134>
- [39]. Correa-Navarro, Y.M., Giraldo, L., and Moreno-Piraj n, J.C., Biochar from Fique Bagasse for Remotion of Caffeine and Diclofenac from Aqueous Solution, *Molecules*, 25(8), 1849, (2020). <https://doi.org/10.3390/molecules25081849>
- [40]. Ge a, M., Wi niewska, M., and Nowicki, P., Biochars and activated carbons as adsorbents of inorganic and organic compounds from multicomponent systems – A review, *Advances in Colloid and Interface Science*, 305, 102687, (2022). <https://doi.org/10.1016/j.cis.2022.102687>
- [41]. Setianingsih, T., Metode Karakterisasi Karbon Nanomaterial, UB Press, Malang, (2023c). [https://books.google.co.id/books?id=ii7oEAAAQBAJ&printsec=frontcover&source=gbg\\_summary\\_r&cad=0#v=onepage&q&f=false](https://books.google.co.id/books?id=ii7oEAAAQBAJ&printsec=frontcover&source=gbg_summary_r&cad=0#v=onepage&q&f=false)
- [42]. Mekuye, B. and Abera, B., Nanomaterials: An overview of synthesis, classification, characterization, and applications, *Nano Select*, 4, 486 – 501, (2023). <https://doi.org/10.1002/nano.202300038>
- [43]. Setianingsih, T., Purwonugroho, D., and Prananto, Y.P., Sintesis Nanokarbon dan Komposit Nanokarbon dari Biomassa dengan Metode Pirolisis Fasa Padat dengan Microwave - Sonikasi untuk Remediasi Lahan Tanah Pertanian Tercemar Pestisida, Laporan Hibah Doktor Lektor Kepala, Brawijaya University, Malang, (2020).
- [44]. Feret, F.R., Determination of The Crystallinity of Calcined and Graphitic Cokes by X-ray Diffraction, *Analyst*, 123, 595 – 600, (1998). <https://doi.org/10.1039/A707845E>
- [45]. Rofikoh, V., Zaman, B., and Samadikun, B.P., The Potential of Commercial Biomass-Based Activated Carbon to Remove Heavy Metals in Wastewater – A Review. *Jurnal Ilmu Lingkungan*, 22(1), 132 – 141, (2024). <https://doi.org/10.14710/jil.22.1.132-141>
- [46]. Ben Abdallah, A., Ben Hassen Trabelsi, A., Navarro, M.V., Navarro, M.V., Veses, A., Garcia, T., and Mihoubi, D., Pyrolysis of tea and coffee wastes: effect of physicochemical properties on kinetic and thermodynamic characteristics, *Journal of Thermal Analysis and Calorimetry*, 148, 2501–2515 (2023). <https://doi.org/10.1007/s10973-022-11878-4>
- [47]. Kelkar, S., Safron, C.M., Chai, L., Bovee, J., Stuecken, T.R., Garedew, M., Li, Z., and Krieger, R.M., Pyrolysis of spent coffee grounds using a screw-conveyor reactor, *Fuel Processing Technology*, 137, 170 – 178, (2015). <https://doi.org/10.1016/j.fuproc.2015.04.006>
- [48]. Murthy, P.S. and Madhava, N.M., Sustainable management of coffee industry by-products and value addition—A review, Sustainable management of coffee industry by-products and value addition - a review, *Resources, Conservation and Recycling*, 66, 45 – 58, (2012). <https://doi.org/10.1016/j.resconrec.2012.06.005>
- [49]. Mahmoud, D.A.R., Allam, M.A., and Farag, M.M., Tea Wastes as An Alternative Sustainable Raw Material for Ethanol Production, *Egyptian Journal of Chemistry*, 63(7), 2683 – 2697, (2020). <https://doi.org/10.21608/ejchem.2020.21785.2293>
- [50]. Rajan, M.J. and Anish, C.L., Role of Activated Carbon in Water Treatment, In: Dincer, S., Takci, H.A.M., and Ozdenefe, M.S., Water Quality - New Perspectives, IntechOpen, London, (2022). <http://dx.doi.org/10.5772/intechopen.108349>
- [51]. Wood, R., Masek, O., and Erastova, V., Developing a molecular-level understanding of biochar materials using public characterization data, *Cell Reports Physical Science*, 5(7), 102036, (2024). <https://doi.org/10.1016/j.xcrp.2024.102036>
- [52]. Gaur, M., Misra, C., Yadav, A.B., Swaroop, S., Maolmhuaidh, F. ., Bechelany, M., and Barhoum, A., Biomedical Applications of Carbon Nanomaterials: Fullerenes, Quantum Dots, Nanotubes, Nanofibers, and Graphene, *Materials*, 14, 5978, (2021). <https://doi.org/10.3390/ma14205978>
- [53]. Siipola, V., Tamminen, T., K lli, A., Lahti, R., Romar, H., Rasa, K., Keskinen, R., Hyv luoma, J., Hannula, M., and Wikberg, H., Effects of biomass type, carbonization process, and activation method on the properties of bio-based activated carbons, *BioResources*, 13(3), 5976 – 6002, (2018). <http://dx.doi.org/10.15376/biores.13.3.5976-6002>
- [54]. Boulanger, N., Talyzin, A.V., Xiong, S., Hultberg, M., and Grimm, A., High surface area activated carbon prepared from wood-based spent mushroom substrate for supercapacitors and water treatment, *Colloids and Surfaces A: Physicochemical and Engineering Aspects*, 680, 132684, (2024). <https://doi.org/10.1016/j.colsurfa.2023.132684>
- [55]. Li, G., Iakunkov, A., Boulanger, N., Lazar, O.A., Enachescu, M., Grimm, A., and Talyzin, A.V., Activated carbons with extremely high surface area produced from cones, bark and wood using the same procedure, *RSC Advances*, 13, 14543, (2023). <https://doi.org/10.1039/D3RA00820G>

- [56]. Jiang, L., Liu, Y., Liu, S., Zeng, G., Hu, X., Hu, X., Guo, Z., Tan, X., Wang, L., and Wu, Z., Adsorption of Estrogen Contaminants by Graphene Nanomaterials under Natural Organic Matter Preloading: Comparison to Carbon Nanotube, Biochar, and Activated Carbon, *Environmental Science & Technology*, 51(11), 6352 – 6359, (2017). <https://dx.doi.org/10.1021/acs.est.7b00073>
- [57]. Fidel, R.B., Evaluation and implementation of methods for quantifying organic and inorganic components of biochar alkalinity, Master of Science Dissertation, Soil Science (Soil Chemistry), Iowa State University, Ames, (2012). <https://dr.lib.iastate.edu/server/api/core/bitstreams/ee00dd56-743f-40bc-9182-bccee1b5f5a8/content>
- [58]. Xiao, F., Bedane, A.H., Mallula, S., Sasi P.C., Alinezhad, A., Soli, D., Hagen, Z.M., and Mann, M.D., Production of granular activated carbon by thermal air oxidation of biomass charcoal/biochar for water treatment in rural communities: A mechanistic investigation, *Chemical Engineering Journal Advances*, 4, 100035, (2020). <https://doi.org/10.1016/j.cej.2020.100035>
- [59]. Hoffmann, V., Jung, D., Zimmermann, J., Correa, C.R., Elleuch, A., Halouani, K., and Kruse, A., Conductive Carbon Materials from the Hydrothermal Carbonization of Vineyard Residues for the Application in Electrochemical Double-Layer Capacitors (EDLCs) and Direct Carbon Fuel Cells (DCFCs), *Materials*, 12(10), 1703, (2019). <https://doi.org/10.3390/ma12101703>
- [60]. Akpasi, S.O., Anekwe, I.M.S., Adediji, J., and Kiambi, S.L., Biochar Development as a Catalyst and Its Application, In: Bartoli, M., Giorcelli, M., and Tagliaferro, A., Biochar - Productive Technologies, Properties and Applications, IntechOpen, London, (2022). <http://dx.doi.org/10.5772/intechopen.105439>
- [61]. Ghorbani, M., Amirahmadi, E., Neugschwandtner, R.W., Konvalina, P., Kopecký, M., Moudrý, J., Perná, K., and Murindangabo, Y.T., The Impact of Pyrolysis Temperature on Biochar Properties and Its Effects on Soil Hydrological Properties, *Sustainability*, 14(22), 14722, (2022). <https://doi.org/10.3390/su142214722>
- [62]. Chatterjee, R., Sajjadi, B., Chen, W.Y., Mattern, D.L., Hammer, N., Raman, V., and Dorris A., Effect of Pyrolysis Temperature on PhysicoChemical Properties and Acoustic-Based Amination of Biochar for Efficient CO<sub>2</sub> Adsorption, *Frontiers in Energy Research*, 8, 85, (2020). <https://doi.org/10.3389/fenrg.2020.00085>
- [63]. Lan, X., Jiang, X., Song, Y., Jing, X., and Xing, X., The effect of activation temperature on structure and properties of blue coke-based activated carbon by CO<sub>2</sub> activation, *Green Processing and Synthesis*, 8(1), 837 – 845, (2019), <https://doi.org/10.1515/gps-2019-0054>
- [64]. Kopeć, M., Baran, A., Mierzwa-Hersztek, M., Krzysztof, G., and Chmiel, M.J., Effect of the Addition of Biochar and Coffee Grounds on the Biological Properties and Ecotoxicity of Composts, *Waste Biomass Valor*, 9, 1389 – 1398, (2018). <https://doi.org/10.1007/s12649-017-9916-y>
- [65]. Draper, K., The Potential for Biochar to Improve Sustainability in Coffee Cultivation and Processing: A White Paper, Ithaka Institute for Carbon Intelligence, (2018). <https://www.biochar-journal.org/itjo/media/doc/1540017045049.pdf>
- [66]. Barakat, N.A.M., Hamad, A., Bastaweesy, A.M., and Hefny, R.A., Effective Decolorization and Turbidity Removal of Canal Water using Activated Carbon Prepared from Local Agricultural Wastes, *Egypt. J. Chem.*, 66(12), 137 – 148, (2023). <https://doi.org/10.21608/ejchem.2023.156041.6753>
- [67]. El-Khouly, S.M. and Fathy, N.A., A review on nano-carbon materials for pollution remediation, *Egypt. J. Chem.*, 64(12), 7029 – 7052, (2021). <https://doi.org/10.21608/EJCHEM.2021.80926.4007>
- [68]. Kalinke, A.H., Marcolino-Junior, L.H., Bergamini, M.F., and Zarbin, A.J.G., Platinum Nanoparticles Supported by Carbon Nanotubes: Improvement in electrochemical sensor performance for caffeine determination, *An. Acad. Bras. Ciênc.*, 96(1), e20230067, (2024). <https://doi.org/10.1590/0001-3765202420230067>
- [69]. Peng, Z., Liu, X., Zhang, W., Zeng, Z., Liu, Z., Zhang, C., Liu, Y., Shao, B., Liang, Q., Tang, W., and Yuan, X., Advances in the application, toxicity and degradation of carbon nanomaterials in environment: A review, *Environment International*, 134, 105298, (2020). <https://doi.org/10.1016/j.envint.2019.105298>
- [70]. Osman, A.I., Blewitt, J., Abu-Dahrieh, J.K., Farrell, C., Al-Muhtaseb, A.H., Harrison, J., and Rooney, D.W., Production and characterisation of activated carbon and carbon nanotubes from potato peel waste and their application in heavy metal removal, *Environmental Science and Pollution Research*, 26, 37228 – 37241, (2019). <https://doi.org/10.1007/s11356-019-06594-w>
- [71]. Shan, J., Ji, R., Yu, Y., Xie, Z., and Yan, X., Biochar, activated carbon and carbon nanotubes have different effects on fate of <sup>14</sup>C-catechol and microbial community in soil, *Scientific Reports*, 5, 16000, (2015). <https://doi.org/10.1038/srep16000>
- [72]. Qiao, N., Chang, J., Hu, M., and Ma, H., Novel bentonite particle electrodes based on Fenton catalyst and its application in Orange II removal, *Desalination and Water Treatment*, 57(36), 17030 – 17038, (2016). <https://doi.org/10.1080/19443994.2015.1083889>
- [73]. Khan, I., Saeed, K., Zekker, I., Zhang, B., Hendi, A.H., Ahmad, A., Ahmad, S., Zada, N., Ahmad, H., Shah, L.A., Shah, T., and Khan, I., Review on Methylene Blue: Its Properties, Uses, Toxicity and Photodegradation, *Water*, 14(2), 242, (2022). <https://doi.org/10.3390/w14020242>
- [74]. Yang, Y., Sun, F., Li, J., Chen, J., and Tang, M., The effects of different factors on the removal mechanism of Pb(II) by biochar-supported carbon nanotube composites, *RSC Adv.*, 10, 5988, (2020). <https://doi.org/10.1039/c9ra09470a>
- [75]. Quispe, J.I.B., Campos, L.C., Mašek, O., and Bogush, A., Removal of anionic surfactant from aqueous solutions by adsorption onto biochars: characterisation, kinetics, and mechanism, *Environmental Technology*, 45(26), 5723–5744, (2024) <https://doi.org/10.1080/09593330.2024.2304677>
- [76]. Glushkov, D.O., Nyashina, G.S., Anand, R., and Strizhak, P.A., Composition of gas produced from the direct combustion and pyrolysis of biomass, *Process Safety and Environmental Protection*, 156, 43 – 56, (2021). <https://doi.org/10.1016/j.psep.2021.09.039>
- [77]. Madikizela, L.M. and Pakad, V.E., Trends in removal of pharmaceuticals in contaminated water using waste coffee and tea-based materials with their derivatives, *Water Environment Research*, 95(4), e10857, (2023). <https://doi.org/10.1002/wer.10857>

- 
- [78]. Osman, A.I., Farrell, C., Al-Muhtaseb, A.H., Harrison, J., and Rooney, D.W., The production and application of carbon nanomaterials from high alkali silicate herbaceous biomass, *Scientific Reports*, *10*, 2563, (2020). <https://doi.org/10.1038/s41598-020-59481-7>
- [79]. Kumar, M., Xiong, X., Wan, Z., Sun, Y., Tsang, D.C.W., Gupta, J., Gao, B., Cao, X., Tang, J., and Ok, Y.S., Ball milling as a mechanochemical technology for fabrication of novel biochar nanomaterials, *Bioresource Technology*, *312*, 123613, (2020). <https://doi.org/10.1016/j.biortech.2020.123613>